LOW TEMPERATURE PHOTOLUMINESCENCE STUDIES ON SPUTTER DEPOSITED CADMIUM SULPHIDE/CADMIUM TELLURIDE HETEROJUNCTIONS AND SOLAR CELLS

BY

MOHIT TUTEJA

THESIS

Submitted in partial fulfillment of the requirements
for the degree of Master of Science in Materials Science and Engineering
in the Graduate College of the
University of Illinois at Urbana-Champaign, 2014

Urbana, Illinois

Advisor:

Professor Angus Rockett

ABSTRACT

Device quality CdS/CdTe heterostructures and completed solar cells (~12% efficient) have been studied using low-temperature photoluminescence (PL). The PL was studied as a function of temperature (82-295 K) and laser excitation power (0.02-2 mW). The CdS/CdTe junctions were grown on transparent conducting oxide covered soda lime glass using rf-sputter deposition. It was found that the luminescence shifts from being dominated by sub-gap defect mediated emission at lower excitation powers to near band edge excitonic emission at higher excitation powers. The effect of copper (Cu) used in making back contacts was studied in connection with the CdS/CdTe junction PL. It was found that the presence of Cu suppresses the sub-band gap PL emissions. This effect is thought to be either due to Cu occupying cadmium vacancies (V_{Cd}) or forming acceptor complexes with them. This points to a potential role of Cu in plugging sub-band gap recombination routes and hence increasing charge separation ability of the device. An energy band diagram is presented indicating various observed transitions and their possible origins.

To my loving parents, supportive advisor, caring friends…

and the journey through graduate school.

TABLE OF CONTENTS

CHAPTER 1: INTRODUCTION…… 1

1.1: Motivation…….. 1

1.2: Thesis Statement…… 2

1.3: Thesis Summary…… 2

CHAPTER 2: BACKGROUND…… 4

CHAPTER 3: EXPERIMENT……7

CHAPTER 4: RESULTS…… 9

4.1: PL of $CdCl_2$ treated CdTe: Excitation from the CdTe surface……..... 9

4.2: PL from CdS/CdTe junction: Excitation from the glass side (sample A) 11

4.3: PL from CdS/CdTe junction: Excitation from the glass side (sample B) 12

CHAPTER 5: DISCUSSION…… 14

CHAPTER 6: CONCLUSIONS…..……. 17

REFERENCES……. 18

FIGURES…….. 19

CHAPTER 1

INTRODUCTION

1.1 Motivation

In recent years, there has been a shift of focus towards utilizing renewable sources of energy. Rising energy costs and increasing environmental concerns associated with fossil fuels are the major contributing factors. Thin film photovoltaics have emerged as a major renewable energy source with a-Si, GaAs, CdTe and $CuInGaSe_2$ as various competing technologies. These materials exhibit numerous optical and electronic properties that have advantages over the bulk crystalline materials such as Si. Due to their high absorption coefficients ($>10^4$ cm^{-1}) only 1-2 μm of the material are needed to utilize the incoming radiation, as opposed to crystalline silicon where tens of microns are required to obtain similar results [1]. This results in a decrease in the amount of material needed for the thin film devices, which translates to lower costs due to lower materials utilization and processing times. Recently, CdTe based solar cells have demonstrated a record efficiency of 20.4%, making them very promising candidates for economically competitive large-scale power generation.

One of the most important factors limiting the photovoltaic efficiency of a device is the bandgap of the component semiconductor. The semiconductor material is transparent to the fraction of the total solar energy that is lower than its bandgap energy. This loss accounts to about 20% of total solar energy at 1.0 eV bandgap [2]. Further, there is an additional loss due to thermalization of the charge carriers to their respective band edges upon excitation by photons that are above the band edge energy. In addition, all of the recombination mechanisms active within the photon absorber layer impede the

charge separation ability of the solar cell and reduce its efficiency. Recombination is especially important in polycrystalline materials such as CdTe, $CuInGaSe_2$ etc. as the grain boundaries, cation/anion vacancies and intersitials present in these materials may act as efficient recombination centers. This necessitates an investigation into the sub-gap traps/recombination centers present in CdTe that limit the efficiency of the corresponding solar cells.

1.2 Thesis Statement

This thesis applies low temperature photoluminescence (PL) to increase the understanding of recombination of minority charge carriers in CdTe photovoltaics mediated by sub-bandgap defect states. The analysis provides information about various factors limiting the cell efficiency and has a potential to provide methods to enhance device performances.

1.3 Thesis Summary

Brief background information on CdTe solar cells and their PL analysis existing in the literature is provided in **CHAPTER 2**. A description of the experimental procedure used to grow the CdS/CdTe heterojunctions and completed devices used in this study is given in **CHAPTER 3**. This is followed by the description of the setup used for the PL analysis. **CHAPTER 4** is a consolidation of the results obtained from PL performed on the CdS/CdTe heterojunction and CdTe by exciting the front and back of the device respectively. Measurements with and without back contacts are also compared. **CHAPTER 5** contains a discussion of the results obtained, their connection to specific

defects/ electronic transitions and a comparison with the relevant literature. **CHAPTER 6** contains a summary of the work done and conclusions reached.

CHAPTER 2

BACKGROUND

The performance of CdS/CdTe heterojunction devices are primarily governed by various defect-mediated recombinations that are responsible for reducing the effective charge separation. These defect states have mainly been attributed to Cadmium vacancies (V_{Cd}) [3], complexes consisting of V_{Cd} and donor impurities such as Cl [4], copper on cadmium sites (Cu_{Cd}) [5] and donor-acceptor (DA) transitions [6]. Cl is incorporated in the CdTe layer post deposition, presumably in the form of chlorine on tellurium sites (Cl_{Te}), during annealing with $CdCl_2$ vapor. This annealing is found to increase CdTe grain size [7]. Cu is introduced, usually as part of a back contact, and acts to enhance p-type doping of CdTe and improve the ohmic behavior of back contacts [8].

PL is an important technique to probe states in the energy gap of the semiconductor and hence to study the possible carrier trapping and recombination routes. By analysis of the dependence of intensity and spectral position of the sample luminescence on incident laser intensity, wavelength, and sample temperature we can determine the origins of emission lines from the material [9]. Some work has been done on PL based investigation of CdTe films and CdS/CdTe based devices [4,10–12]. Still, unambiguous assignment of various peaks observed in PL spectra is rarely possible. This is partly due to the fact that most solar cells have relatively complex polycrystalline CdTe as their absorber layer. It has been noted that the polycrystalline materials outperform their single crystal counterparts [13]. Due to the presence of various recombination sites in the polycrystalline material the emission lines are broadened, which makes their accurate identification difficult.

The PL spectrum of a semiconductor depends both on the sample temperature and the excitation power of the laser as the band edges and sub-band gap states have a finite capture cross-section, which changes with both of these quantities. The study of various recombination processes occurring in CdTe and at the CdS/CdTe interface is important because it directly influences charge separation and hence V_{OC}. In the present study, low temperature PL has been employed to study the electronic energy levels of the defect states and their corresponding luminescence emission for sputter deposited CdTe solar cells and junctions. Sputter deposition is preferred as it requires lower substrate temperatures (~250^0C) for growth as compared to thermal evaporation techniques. For instance, closed-space sublimation (CSS) requires a temperature of ~600° C for CdTe growth. In addition, sputtering technology is well developed to coat large areas of glass homogenously. However, CSS deposited CdTe solar cells often have higher efficiencies as compared to sputtered devices [14]. In the present study, PL emission from all sputtered CdS/CdTe junctions is investigated and the results are compared to their vapor phase deposited counterparts to investigate the reasons for higher efficiencies of CSS deposited CdTe solar cells.

In order to study these recombination processes, I have carried out experiments with the excitation from the CdTe surface side and the glass/CdS side of the junction so as to probe the electronic properties of the CdTe surface and the CdS/CdTe junction, respectively. The resulting PL spectra were measured as a function of temperature (80-295 K) and excitation power (0.02 -2 mW). PL from the heterojunction was measured both after $CdCl_2$ treatment and after completing the device by depositing back contacts for the purpose of making a comparison with the data on evaporated materials and to

study the effect of Cu on luminescence properties.

The current study extends previous work with a more detailed characterization of the temperature and power dependence of luminescence peaks. Overall the PL spectra obtained agree with the reported spectra. However, a shift is observed in the PL emission from being dominated by sub-band gap defect mediated emission at lower excitation powers to near band edge emission at higher excitation powers. As seen from the PL spectra, the presence of Cu as a dopant is found to suppress the sub-gap luminescence and might actually promote band-to-band recombination. This points to the Cu diffusion from the CdTe surface to CdS/CdTe junction and its effect on carrier recombination.

CHAPTER 3

EXPERIMENT

The samples studied here were grown at University of Toledo on NSG-Pilkington TEC-15 glass substrates, which is a soda lime glass coated with a transparent conductive oxide layer. The CdS and CdTe were sequentially deposited by magnetron sputtering at a substrate temperature of 250° C, an rf power of 200 W, and an Ar pressure of 15 mTorr and 10 mTorr for CdS and CdTe depositions, respectively. The CdS and CdTe thicknesses were 120 nm and 2200 nm, respectively, as monitored *in-situ* using real time spectroscopic ellipsometry. Following this deposition the samples were $CdCl_2$ heat treated by applying a saturated aqueous solution to the CdTe film surface and annealing in dry air for 30 min at 387° C. One sample (sample A) was taken out at this stage and the other sample (sample B) was coated with Cu/Au bilayer contacts of 3/30 nm thicknesses. Sample B was subsequently annealed at 150° C in air for 45 min.

The PL studies were carried out at University of Illinois. The samples were mounted on a temperature-controlled vacuum cryostage and illuminated with a 532 nm Nd:YAG laser with a peak power of less than 50 mW. Photons of this wavelength are absorbed strongly (absorption coefficient > 80,000 cm^{-1} at room temperature) in CdTe and very weakly (absorption coefficient ~ 0) in CdS. The maximum power delivered to the sample was ~11 mW. The excitation power was varied using an adjustable neutral density filter. A Princeton Instruments grating-based monochromator (Spectra-Pro 300i) coupled with a Si CCD detector (PIXIS 100) was used for signal detection. The sample was cooled down to 82 K in a Kadel Engineering Corp. dewar. The typical range of measurement temperatures was 82–295 K, regulated using a LakeShore cryotronics 330

autotune temperature controller. PL spectra were obtained by exciting the sample from the glass side to probe CdS/CdTe junction in the case of samples A and B and from the CdTe surface side to probe CdTe bulk characteristics in the case of sample A. Both samples (A and B) had an area of 1 cm x 1 cm and the laser spot was 0.2 mm^2 in area. The completed device (sample B) used for this study had an open circuit voltage (V_{OC}) ~ 0.8 V, short circuit current (J_{SC}) ~ 22 mA/cm^2 and was ~12% efficient.

CHAPTER 4

RESULTS

4.1 PL of $CdCl_2$ treated CdTe: Excitation from the CdTe surface

The PL spectra obtained at various temperatures by exciting the CdTe side of the $CdCl_2$-treated, uncontacted CdS/CdTe junction sample are shown in Fig. 1(a). Here the excitation power is ~0.7 mW. Fig. 1(b) shows a 2D contour plot of the PL spectra obtained at 82 K at different excitation powers. The excitation power range was 0.02 to 1.55 mW and the interval between measured spectra is ~ 0.1 mW. Taken together, the data in Fig. 1 shows that the 82 K spectrum consists of two prominent bands centered at ~1.42 and ~1.55 eV. The 1.42 eV sub-bandgap transition is dominant at low excitation powers up to ~0.7 mW and the near band gap 1.55 eV transition band becomes dominant at higher excitation powers and has a distinct shoulder around 1.58 eV.

In order to calculate the relative intensities of various emission processes to identify their origin, the spectra is peak fit as follows. The 1.42 eV transition in 82 K spectra as shown in Fig. 1(a) is fit with an assymetric Gaussian function, the peak at 1.55 eV is fit with a Lorentzian function and the shoulder at 1.58 eV is fit with an exponentially modified Gaussian function following the approach of Hernandez et al. [15]. In the interest of saving computation time the 1.58 eV transition was modeled as an exponentially modified Gaussian rather than the integral as in [15], as both share a similar peak shape. Fig. 2(a) shows the variation of the 1.42 eV and 1.55 eV band integrated luminescences as a function of excitation power at 82 K. The intensity data are well described by

$$I_{PL} = C\, I_L^k \qquad (1)$$

where I_{PL} is the measured luminescence, I_L is the incident laser power and C is a constant. The values of k obtained from the curve fit are 0.6 ± 0.1 and 2.0 ± 0.4 for 1.42 eV and 1.55 eV transitions, respectively. The errors in k values are determined per a 95% confidence interval. According to Schmidt et al. [16], donor-acceptor (DA) and free to bound (FB) transitions have $k<1$ and excitonic (X) transitions have $1< k<2$. This points to the 1.42 eV and 1.55 eV emissions being DA/FB and X transitions, respectively. Similar k values were obtained upon analysis of the luminescence at other temperatures in range of 82-140 K.

It can be observed from Fig. 1(a) that the 1.42 eV transition luminescence dies out as the measurement temperature is increased from 82 K to 295 K. The decay of this luminescence with temperature (shown in Fig. 2(b)) allows me to calculate the activation energy for this process. The functional relationship between the integrated luminescence and temperature for the linear region in Fig. 2(b) can be modeled using

$$I(T) = A \exp(\Delta E/k_B T) \qquad (2)$$

where I(T) is the temperature dependent integrated luminescence of 1.42 eV band and ΔE is the activation energy for this emission process. This behavior is observed for temperatures above 100 K and gives $\Delta E = 90\pm10$ and 100 ± 10 meV at an excitation power of ~0.5 and ~0.9 mW respectively.

Upon analyzing the variation of the peak position of the 1.58 eV transition as a function of temperature at ~0.5 mW excitation power, we obtain a temperature coefficient of $-(3.1\pm0.5) \times 10^{-4}$ eV/K. This value is close to the value of -3.0×10^{-4} eV/K, as found by Camassel et al. [17] for the temperature coefficient of band gap variation in

CdTe. Thus, the change in position of 1.58 eV transition corresponds the band edge change as temperature is varied.

4.2 PL from CdS/CdTe junction: Excitation from the glass side (sample A)

The PL spectra obtained from the CdS/CdTe junction (sample A) via laser excitation from the glass side at various temperatures are shown in Fig. 3(a). The excitation energy used was ~0.9 mW. Also, a 2D contour plot obtained at 82 K for various excitation powers is shown in Fig 3(b). The PL spectra in Fig. 3(b) have a broad emission band located in the 1.3-1.4 eV region and a peak at 1.55 eV similar to the case of CdTe PL (Fig. 1(b)) as measured from the rear. It can be seen from Fig. 3(b) that the spectra are dominated by the broad emission in the 1.3-1.4 eV region at lower excitation powers up to ~0.3 mW and the sharp 1.55 eV peak at higher excitation powers.

Fig. 4(a) shows the integrated luminescence of the two transitions in the 1.3-1.4 eV region and at 1.55 eV as a function of excitation power at 82 K. These are calculated by fitting the 1.3-1.4 eV transition and 1.55 eV transition with an assymetric Gaussian and a Lorentzian curve respectively. The straight lines are fits to the data as per Equation (1). From this, I find k = 0.79±0.05 and 2.9±0.3 for these two transitions, respectively. The error estimates are based on 95% confidence intervals. As in Fig 1., the k value indicates that the broad peak in 1.3-1.4 eV region is a result of DA/FB recombination. However, k = 2.9 is greater than the limit for excitonic recombination as per [16] and the origin of this discrepancy is unclear at present. Fig. 4(b) shows the variation of the peak positions for the two transitions in Fig. 3(b) with the excitation power at 82 K. Both emission maxima undergo linear blue shift with increasing excitation power before saturating at their final value of ~1.39 and ~1.55 eV, respectively.

Using Equation (2) and following the same process as in Fig. 2(b), I determined the activation energy for the sub-band gap 1.3-1.4 eV transition to be ~110±10 meV at ~0.9mW excitation power. The temperature dependence of the peak position of the 1.55 eV emission as measured at ~0.9 mW excitation power gives a temperature coefficient of $-(3.4\pm0.2) \times 10^{-4}$ eV/K.

4.3 PL from CdS/CdTe junction: Excitation from the glass side (sample B)

Fig. 5(a) shows the CdS/CdTe heterojunction PL spectra as obtained by exciting the sample with Cu-containing back contacts (sample B) from the glass side for ~(0.6-0.9) mW excitation at various temperatures, as listed in the figure. This is different from the case in Fig. 3 in that Cu has been introduced from the back contact. The 82 K spectra consists of a broad sub-bandgap emission with peak at 1.41 eV and a sharp peak at 1.56 eV. Fig. 5(b) is a 2D contour plot, similar to Fig. 1(b), of PL spectra and excitation power as obtained from the CdS/CdTe heterojunction at 82 K. It is clear that for all temperatures and excitation powers the sharp peak at 1.56 eV is the dominant transition. Thus, due to Cu incorporation, the sub-bandgap emission is suppressed and can be only observed up to 120 K, as seen in Fig. 5(b). The 1.58 eV shoulder at 82 K is also absent here, as evident from comparing Fig. 5(a) to Fig. 1(a). Only at 295 K when the emission is broad, is it possible that there is some contribution present from it.

Fig. 6 shows the variation of the 1.41 eV sub-gap and ~1.56 eV integrated peak luminescence with respect to excitation power. As per equation (1) the values of k were found to be 0.90 ±0.12 and 1.9±0.3 for the two transitions, respectively. The error estimates are based on 95% confidence intervals. Thus, I conclude, as in other

measurements, that the sub-gap transition is likely a DA or FB transition and the ~1.56 eV transition is an X transition [16]. The temperature dependence of the peak position of the X emission gives a temperature coefficient of $-(3.7 \pm 0.4) \times 10^{-4}$ eV/K.

CHAPTER 5

DISCUSSION

The temperature dependent PL spectra obtained at fixed excitation power from CdTe, CdS/CdTe interface (with and without back contacts) are shown in Figs. 1(a), 3(a) and 5(a) respectively. All the observed spectra share a similar overall shape. The two characteristic emissions in all PL spectra are the sub-band gap DA/FB emissions and the near band edge excitonic emissions. These are observed in the 1.3-1.4 eV region and around 1.55 eV respectively, in the 82 K PL spectra. The studies on luminescence properties of CdTe [4,6,18] and device quality CdS/CdTe heterojunctions [5,12,19] have reported similar peaks. For instance, a 1.42 eV peak in CdTe PL spectrum has been associated with DA transition involving Cl_{Te}-V_{Cd} defect complex [20]. An acceptor binding energy of 120 meV has been calculated for Cl_{Te}-V_{Cd} defect complex [21]. These are consistent with our calculations that suggest this transition is a DA transition with activation energies of 100 ± 10 and 110 ± 10 meV, as shown in section 4.1 and 4.2 respectively. In addition the near band edge excitonic emssions have also been observed and are associated to acceptor bound excitons [10,15,22]. These similarities between the PL spectra obtained and those observed by others serves to show that the sputtered CdTe based devices have comparable electronic transitions that occur during the device operation. Hence, we can generalize the results obtained from this study to apply to both sputtered and evaporated devices.

The near band edge emissions in Figs. 1(b) and 3(b) both have peaks centered at 1.55 eV and a shoulder towards higher energies. The 1.55 eV peak corresponds to an acceptor bound excitonic emission, which indicates that both these peaks are due to excitons

bound to same acceptor. The dominant acceptor in CdTe is V_{Cd}-Cl_{Te} defect complex. When Cu is introduced (sample B) via the back contact, the luminescence properties of CdS/CdTe junction are affected. As can be seen from Fig. 5(b), the X peak now moves to 1.56 eV from 1.55 eV as seen in Figs. 1(b) and 3(b). This can be explained if this peak is an acceptor bound excitonic emission. Since, after the introduction of Cu in the sample Cu_{Cd} is the primary acceptor [22].

The sub-bandgap transitions observed in the 1.3-1.4 eV region are found to be involving the V_{Cd}-Cl_{Te} defect complex as acceptor. The DA/FB nature of this transition is shown by finding the k value as per Equation (1) and the acceptor state is determined by calculating the activation energies for this transition as per sections 4.1 and 4.2. The thermal quenching of this recombination is caused mainly by thermal excitation of electrons from the valence band into the acceptor level as temperature increases. On comparing Figs. 1(b), 3(b) with Fig. 5(b), it is seen that the sub-bandgap transitions are affected by addition of Cu in the case of sample B. The sub-band gap transition luminescence from CdS/CdTe junction is suppressed upon addition of Cu, whereas Cu is added in the form of 3 nm thick layer on the CdTe surface. This suppression can be explained by investigating the Cu incorporation into CdTe. Upon annealing, Cu is incorporated in CdTe as Cu interstitials (Cu_i) [23], a fast diffusing donor species that interacts with V_{Cd} to form a Cu_i-V_{Cd} acceptor complex, copper on V_{Cd} (Cu_{Cd}) acceptors and Cu_{Cd}-Cu_i neutral complexes [24]. It is likely that the interaction of Cu_i with V_{Cd} to form Cu_{Cd} or Cu_i-V_{Cd} disrupts the Cl_{Te}-V_{Cd} acceptor complex and hence strongly attenuates the DA/FB transition that is observed in PL from samples without Cu incorporation (Fig. 1(a) and 3(a)), which is a result of transition involving V_{Cd}-Cl_{Te}

complex. According to Romero et al. [19], Cu_{Cd} acceptors are recombination centers of much higher efficiencies than any other defect complex involving Cu. It is likely that the remaining sub-bandgap transition as seen in Fig. 5(a) at low temperatures (< 120 K) is due to a transition involving Cu_{Cd}.

On comparison of Figs. 1(b), 3(b) and 5(b), it is noticed that there is a marked transition in the PL spectra from being dominated by sub-band gap DA/FB transition to near band edge X transitions as the excitation power is increased. This is observed at ~0.7, ~0.3 mW in the case of Figs. 1(b) and 3(b) respectively. In the case of CdS/CdTe junction PL spectra from sample B (Fig. 5(b)), the near band edge luminescence is dominant for all excitation powers. This can be traced back to the presence of Cu in sample B, which suppresses the sub-bandgap luminescence. One possible reason for this shift in the dominant luminescence with excitation power could be a larger carrier lifetimes for DA/FB than the X transitions. So, as we increase the carrier generation rate by increasing the excitation power, the rate of recombination via the sub-bandgap transitions is not sufficient to recombine all the generated carriers and the near band edge emissions result. However, further work in this direction is needed before any conclusive statement can be made.

CHAPTER 6

CONCLUSIONS

In the present study, the low temperature PL from CdTe surface and CdS/CdTe junction is measured. The lineshape analysis of the PL spectra reveals that dominant emissions arise from DA, bound exciton and B-B recombination, which are verified by analyzing their respective luminescene with excitation power. The observed transitions are summarized in Fig. 7 in the form of an energy diagram depicting various defect levels and their corresponding emissions. The acceptor level for DA emission observed in PL spectra of CdTe and CdS/CdTe junction without Cu incorporation is identified as Cl_{Te}-V_{Cd} complex based on the activation energy for the emission. It is observed that the B-B recombination is absent in CdS/CdTe junction PL spectra as compared to CdTe. Upon Cu incorporation, the DA transition is suppressed in the CdS/CdTe junction PL spectra due to Cu occupying V_{Cd}. The residual sub-bandgap transition is possibly due to Cu_{Cd} acceptor impurity. The shift in the dominant luminescence from sub-bandgap to near band edge transition as a function of laser excitation power is shown. Further work is required to ascertain the reason for this shift.

REFERENCES

[1] A. Shah, P. Torres, R. Tscharner, N. Wyrsch, and H. Keppner, Science **285**, 692 (1999).

[2] A. L. Fahrenbruch and R. H. Bube, *Fundamentals of Solar Cells : Photovoltaic Solar Energy Conversion / Alan L. Fahrenbruch, Richard H. Bube* (Academic Press, New York, 1983).

[3] T. Okamoto, A. Yamada, and M. Konagai, Thin Solid Films **387**, 6 (2001).

[4] D. . Halliday, J. . Eggleston, and K. Durose, J. Cryst. Growth **186**, 543 (1998).

[5] S. Vatavu, H. Zhao, I. Caraman, P. Gaşin, and C. Ferekides, Thin Solid Films **517**, 2195 (2009).

[6] T. Taguchi, J. Shirafuji, and Y. Inuishi, Jpn. J. Appl. Phys. **12**, 1558 (1973).

[7] H. R. Moutinho, M. M. Al-Jassim, D. H. Levi, P. C. Dippo, and L. L. Kazmerski, J. Vac. Sci. Technol. A **16**, 1251 (1998).

[8] H. C. Chou, A. Rohatgi, E. W. Thomas, S. Kamra, and A. K. Bhat, J. Electrochem. Soc. **142**, 254 (1995).

[9] N. C. Giles-Taylor, R. N. Bicknell, D. K. Blanks, T. H. Myers, and J. F. Schetzina, J. Vac. Sci. Technol. A **3**, 76 (1985).

[10] J. Aguilar-Hernández, G. Contreras-Puente, J. M. Figueroa-Estrada, and O. Zelaya-Angel, Jpn. J. Appl. Phys. **33**, 37 (1994).

[11] Z. C. Feng, A. Mascarenhas, and W. J. Choyke, J. Lumin. **35**, 329 (1986).

[12] D. Grecu and A. D. Compaan, Appl. Phys. Lett. **75**, 361 (1999).

[13] I. Visoly-Fisher, S. R. Cohen, A. Ruzin, and D. Cahen, Adv. Mater. **16**, 879 (2004).

[14] B. E. McCandless and J. R. Sites, in *Handb. Photovolt. Sci. Eng.*, edited by A. Luque and S. Hegedus (John Wiley & Sons, Ltd, 2011), pp. 600–641.

[15] J. Aguilar-Hernandez, G. Contreras-Puente, H. Flores-Llamas, H. Yee-Madeira, and O. Zelaya-Angel, J. Phys. Appl. Phys. **28**, 1517 (1995).

[16] T. Schmidt, K. Lischka, and W. Zulehner, Phys. Rev. B **45**, 8989 (1992).

[17] J. Camassel, D. Auvergne, H. Mathieu, R. Triboulet, and Y. Marfaing, Solid State Commun. **13**, 63 (1973).

[18] S. Vatavu, H. Zhao, V. Padma, R. Rudaraju, D. L. Morel, P. Gaşin, I. Caraman, and C. S. Ferekides, Thin Solid Films **515**, 6107 (2007).

[19] M. J. Romero, D. S. Albin, M. M. Al-Jassim, X. Wu, H. R. Moutinho, and R. G. Dhere, Appl. Phys. Lett. **81**, 2962 (2002).

[20] T. Okamoto, Y. Matsuzaki, N. Amin, A. Yamada, and M. Konagai, Jpn. J. Appl. Phys. **37**, 3894 (1998).

[21] D. M. Hofmann, P. Omling, H. G. Grimmeiss, B. K. Meyer, K. W. Benz, and D. Sinerius, Phys. Rev. B **45**, 6247 (1992).

[22] K. M. James, J. L. Merz, and C. E. Jones, J. Vac. Sci. Technol. A **6**, 2664 (1988).

[23] K. K. Chin, T. A. Gessert, and S.-H. Wei, in *2010 35th IEEE Photovolt. Spec. Conf. PVSC* (2010), pp. 001915–001918.

[24] G. Zoth, F. G. Ridel, and W. Schröter, Phys. Status Solidi B **172**, 187 (1992).

FIGURES

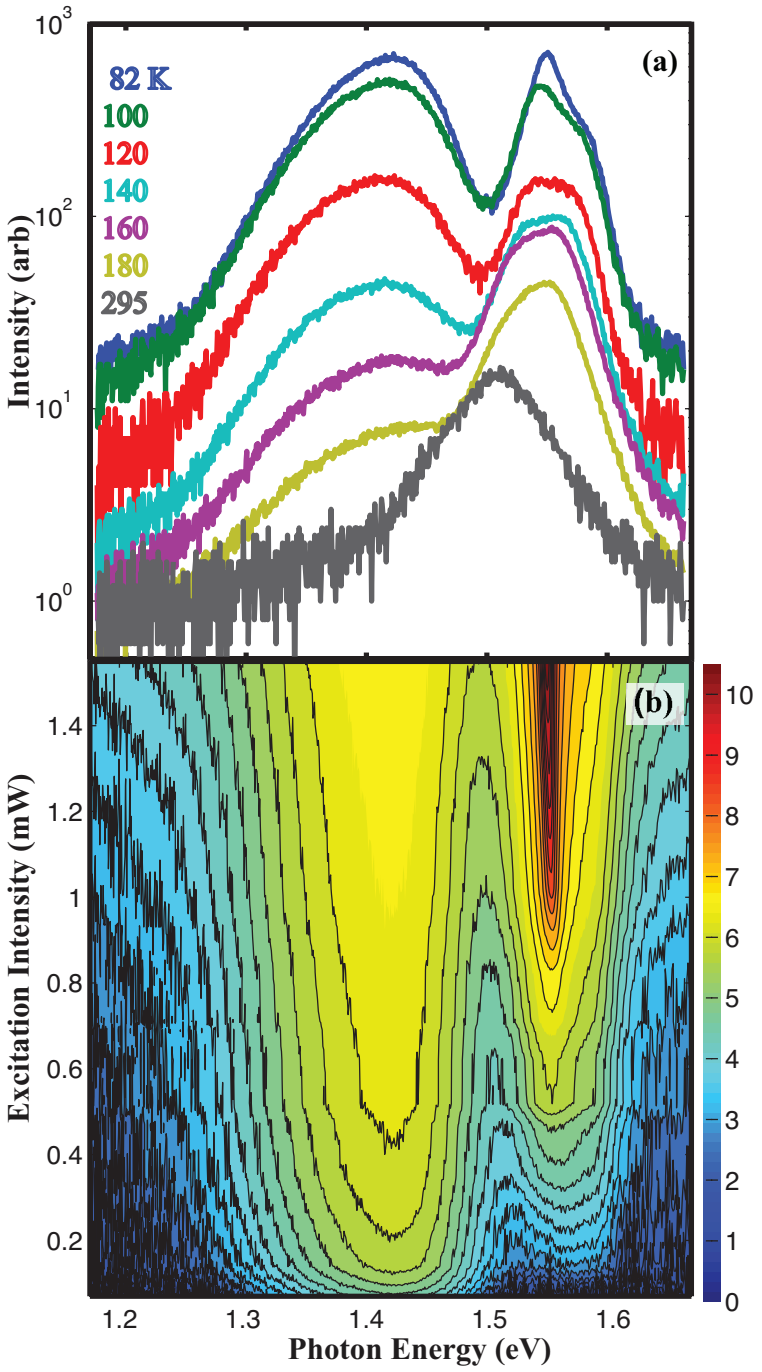

Fig. 1. PL spectra obtained by exciting CdTe surface (sample A) at (a) ~0.7mW laser excitation power as a function of measurement temperature (b) 82K as a function of excitation power of laser

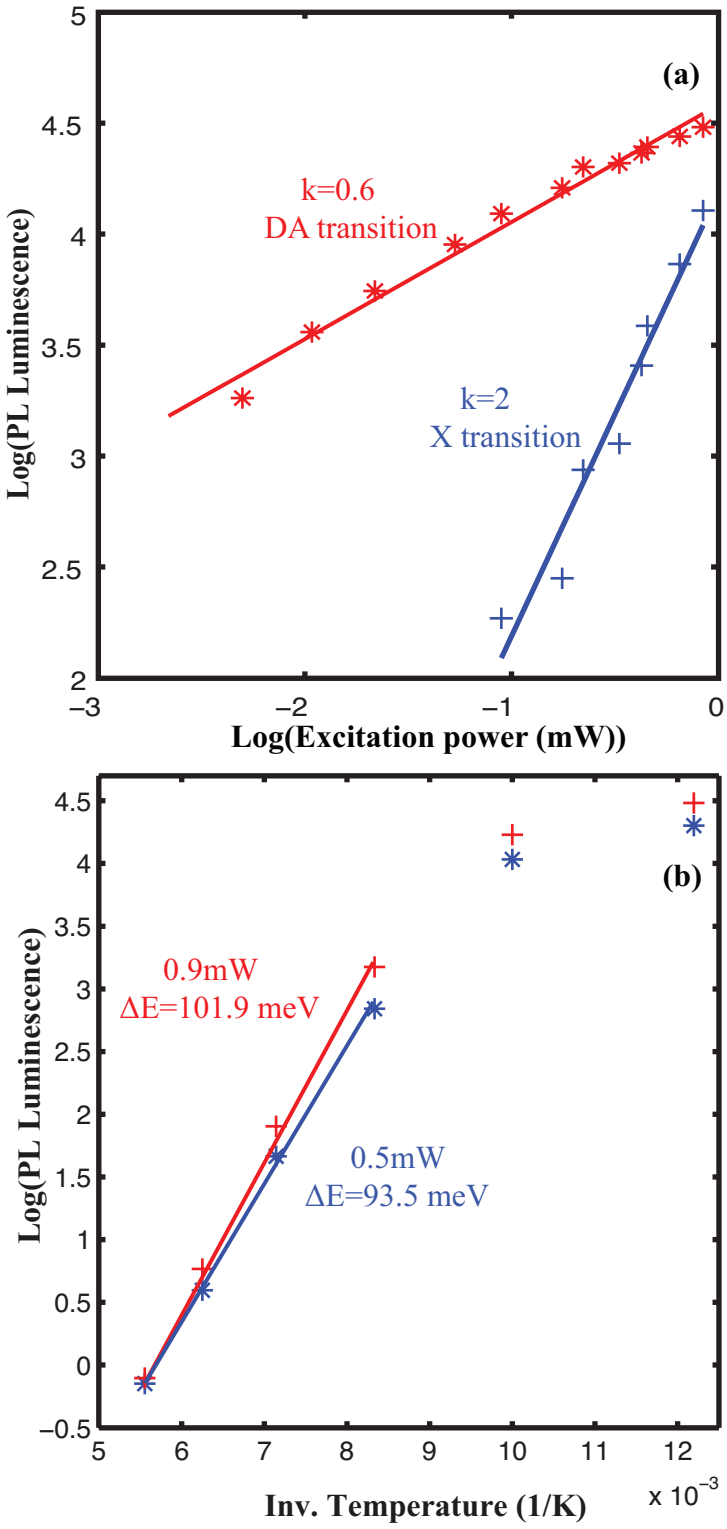

Fig. 2. Plot of (a) DA and X emission luminescence vs. excitation power (b) DA luminescence vs. inverse temperature, in CdTe PL spectra (sample A). The excitation powers used and activation energies obtained are as indicated. Straight lines represent least squares fit to data as per equation (1) and (2) in (a) and (b) respectively.

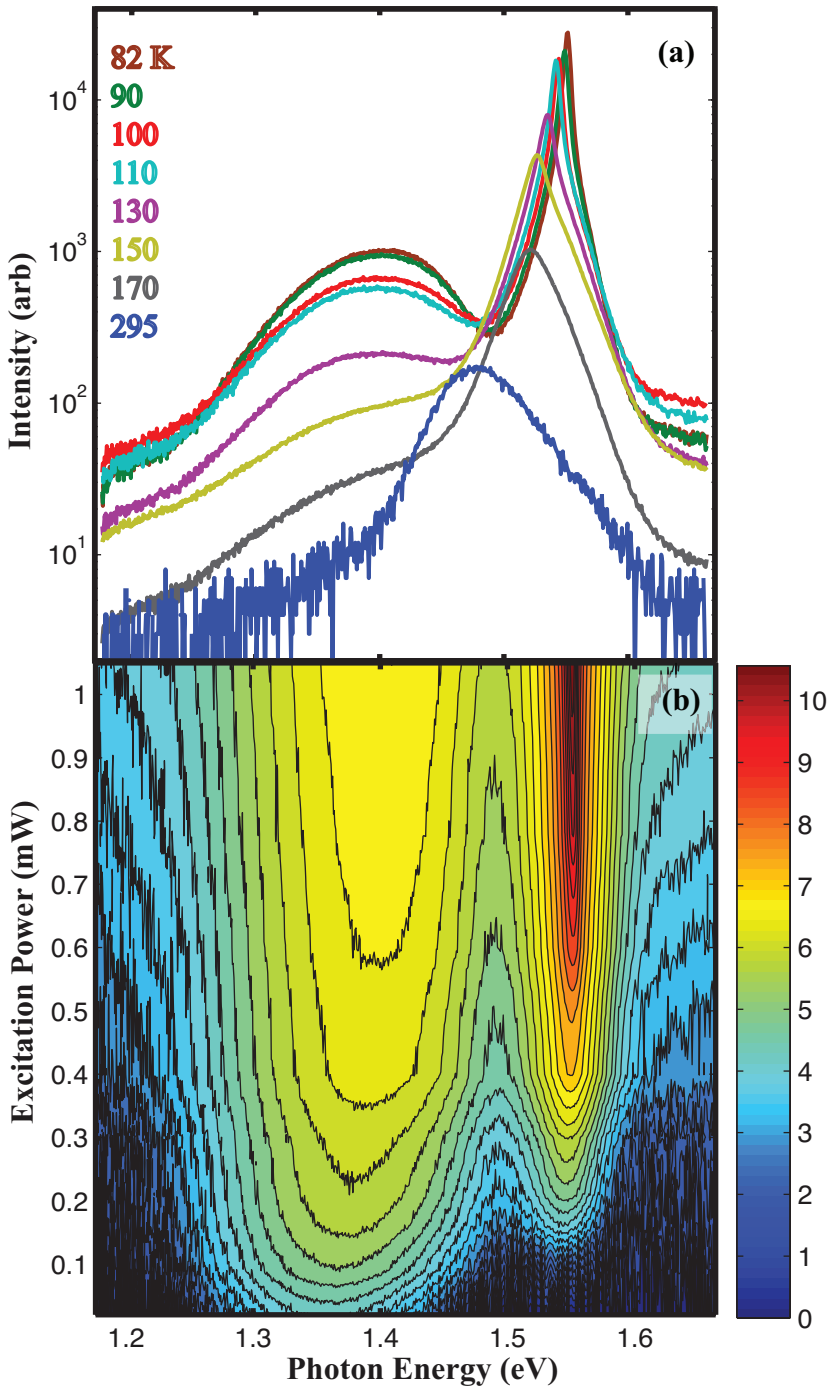

Fig. 3. PL spectra obtained by exciting CdS/CdTe junction (sample A) from glass side at (a) ~0.9mW laser excitation power as a function of measurement temperature (b) 82 K as a function of excitation power of laser

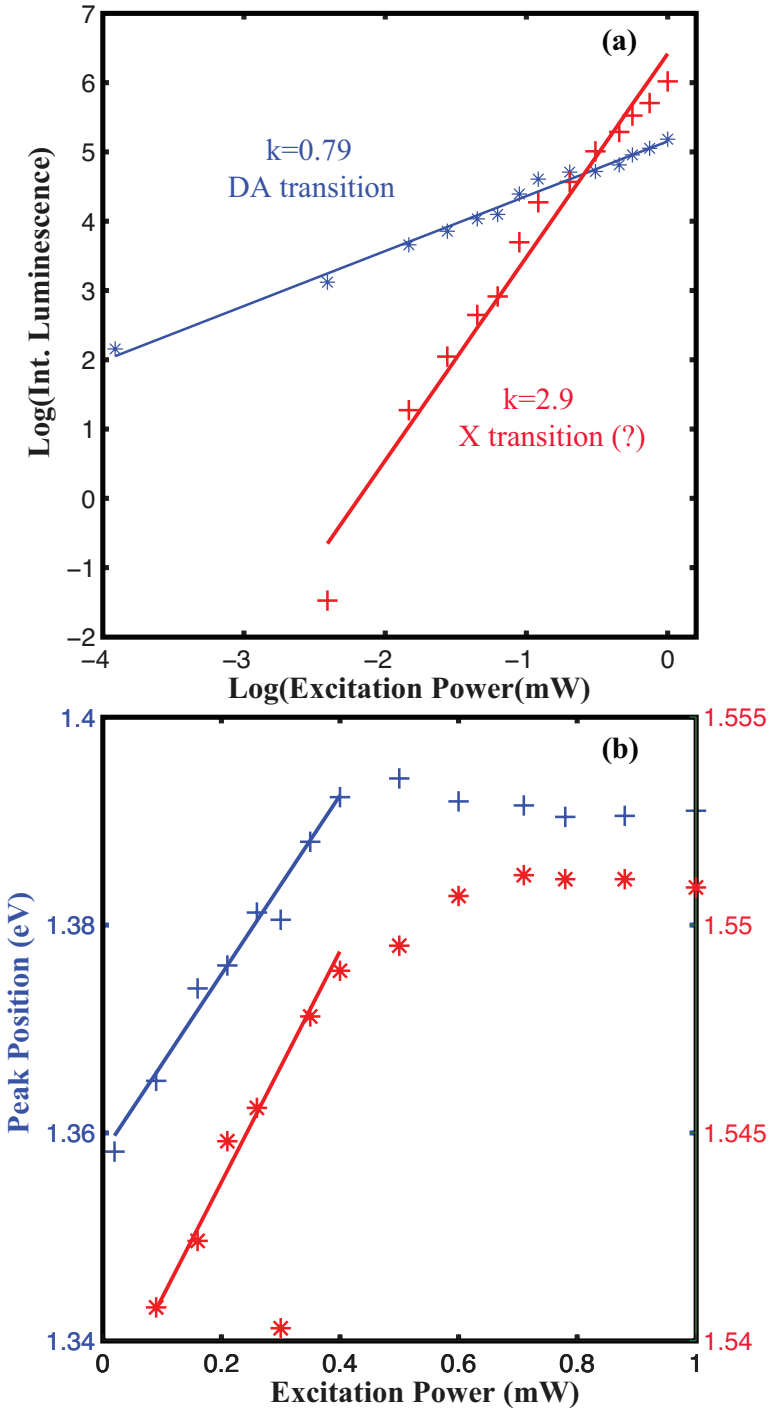

Fig. 4. Plot of (a) DA and X emission luminescence vs. excitation power (b) DA and X emission maxima position vs. excitation power, for sample A in case of CdS/CdTe junction PL. The solid lines are least squares fit to the data as per equation (1) in (a).

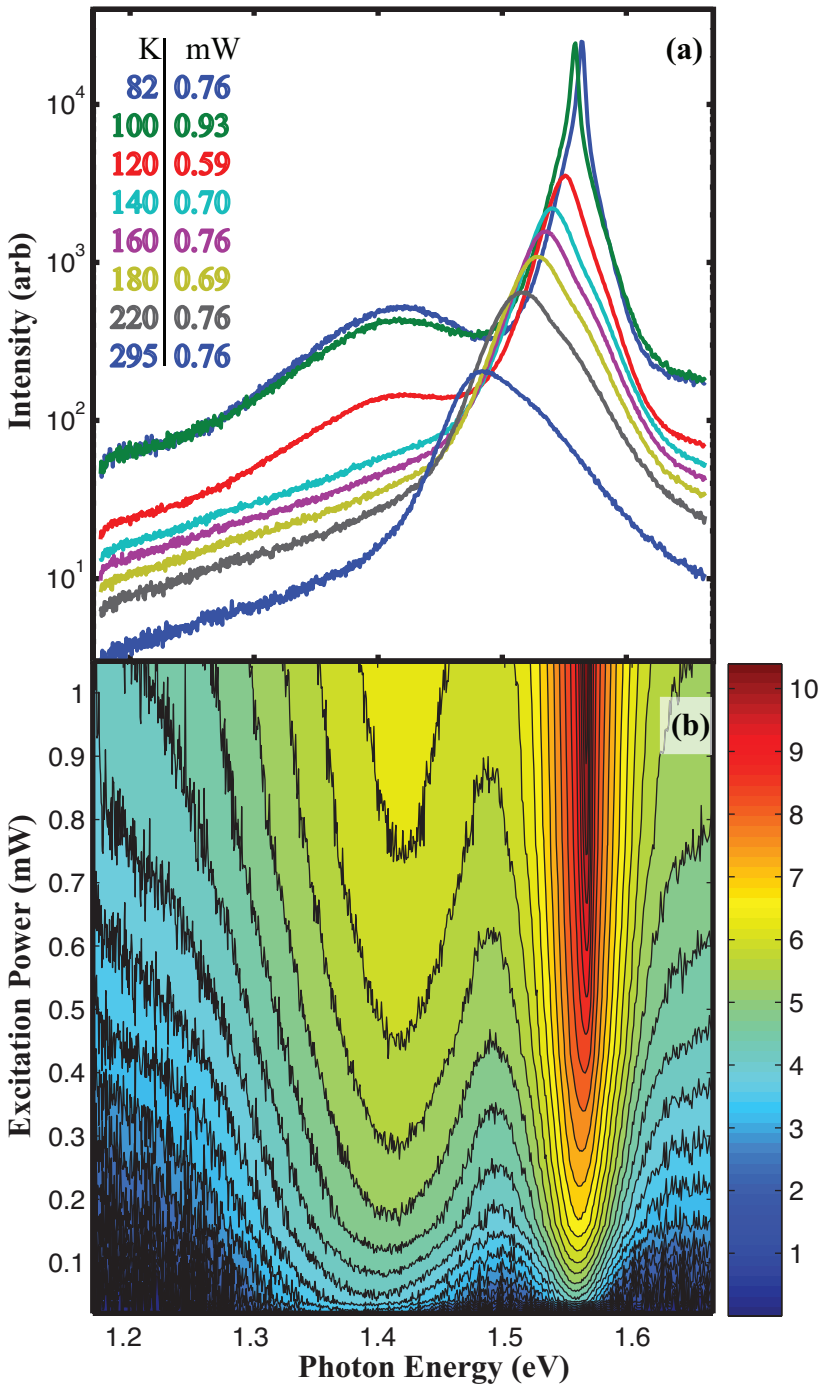

Fig. 5. PL spectra obtained by exciting CdS/CdTe junction from glass side for sample B at (a) 0.6-0.9mW (as labeled) laser excitation power as a function of measurement temperature (b) 82 K as a function of excitation power of laser

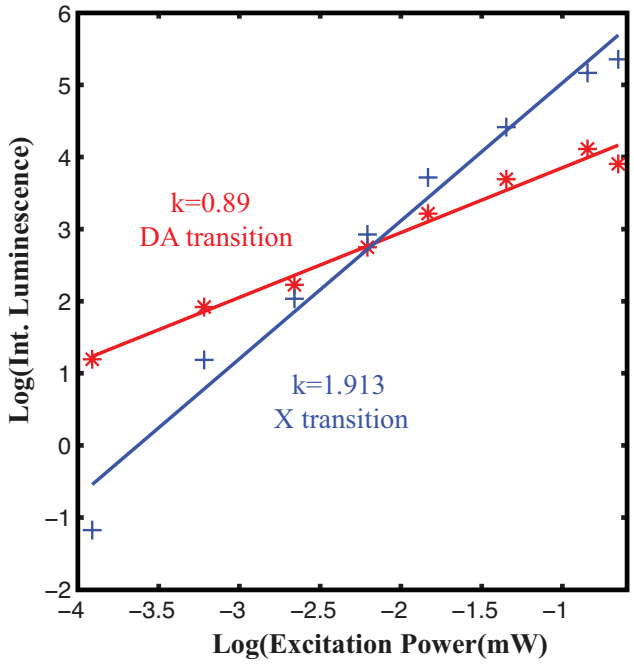

Fig. 6. Plot of DA and X emission luminescence vs. excitation energy for CdS/CdTe junction PL from sample B. Straight lines are least squares fit to data as per equation (1).

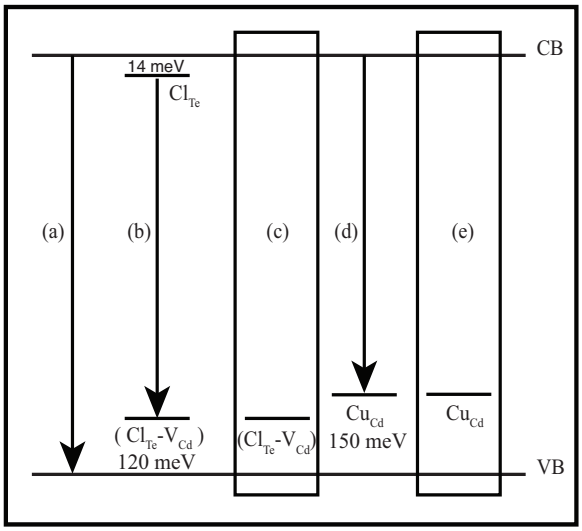

Fig. 7. A suggested energy band diagram showing various defect levels and possible transitions that lead to the observed PL specra. (a) B-B recombination (b) DA transition between Cl_{Te} donor and ($Cl_{Te}V_{Cd}$) acceptor (c) ($Cl_{Te}V_{Cd}$) acceptor bound exciton (d) free to bound transition between CB and Cu_{Cd} level (e) Cu_{Cd} acceptor bound exciton. The binding energy values are written above the donor levels and below the acceptor levels. These values are taken from references cited in the text.

`